

Dual-metal-gate Structure of AlGa_N/Ga_N MIS HEMTs Analysis and Design

Mr. Gaurav Phulwari¹, Mr. Manish Kumar²

Electronics & Communication Engineering^{1,2}, Bhagwant University, Ajmer^{1,2}

M.Tech Scholar¹, Assistant Professor²

Email: er.gauravphulwari@gmail.com¹, mk1038@gmail.com²

Abstract- This paper analyzes the result of a dual-metal-gate structure on the electrical characteristics of AlGa_N/Ga_N metal-insulator-semiconductor high lepton quality transistors. These structures have two gate metals of different work function values (ϕ), with the metal of higher ϕ in the source-side gate, and the metal of lower ϕ in the drain-side gate. As a result of the different ϕ values of the gate metals in this structure, each the electrical field and lepton rate within the channel become higher distributed. For this reason, the trans-conductance, current collapse development, breakdown voltage, and frequency characteristics square measure improved. During this work, the devices were designed and analyzed employing a 2nd technology package simulation tool.

IndexTerms-AlGa_N/Ga_N, 2-DMG, metal-insulator-semiconductor (MIS), high electron mobility transistor (HEMTs), 2D technology computer-aided design (2D-TCAD)

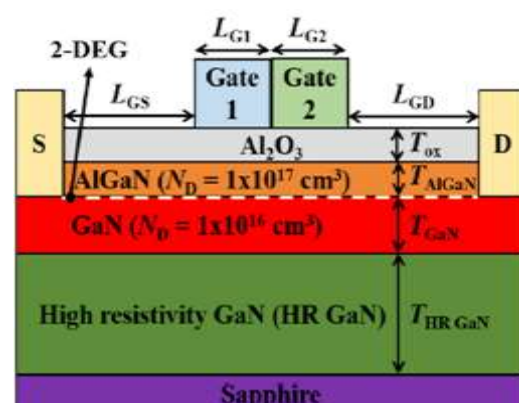
1. INTRODUCTION

Wide band gap power devices for dynamical and high-frequency applications are the topic of a lot of analysis, due to their quality in applications admires air-con, electrical vehicles, national defence radars, and satellite communications. In fact, getting high important electrical fields and high on-current levels has become a very important issue in power physical science devices [7-10]. As a result, AlGa_N/Ga_N heterostructure field-effect transistors (HFETs) are recognized as promising candidates for dynamical and high-frequency applications, due to their outstanding physical and material properties, admire wide band gap, high lepton rate, and high carrier density of their two-dimensional lepton gas (2-DEG). However, AlGa_N/Ga_N HFETs with a Schottky-barrier gate suffer from dynamic power loss, as a result of the big positive gate bias leads to an oversized gate current. To cut back the gate current, analysis on AlGa_N/Ga_N-based metal-insulator-semiconductor (MIS) high lepton quality transistors (HEMTs) has been conducted. The AlGa_N/Ga_N MIS HEMTs gate current has been reduced by victimization gate insulation layer materials admire Si₃N₄, SiO₂, and Al₂O₃, HfO₂ [11-14].

To improve the breakdown voltage (BV), Tran's conductance (g_m), and current collapse development, a lot of analysis has been conducted on a way to effectively distribute the electrical field [2-15] on these devices. One approach to realize Associate in nursing adequate field of force distribution within the channel is that the use of a dual-metal-gate (DMG) structure rather than a single-metal gate (SMG) structure [3-5]. During this work, AlGa_N/Ga_N MIS HEMTs with a DMG structure will be used; the metal

used for the source-side gate metal will have a higher work function (ϕ) than the metal used for the drain-side gate. These AlGa_N/Ga_N MIS HEMTs with a DMG structure are going to be analyzed in terms of

metric weight unit, current collapse development, important field of force, and oftenness (RF) characteristics admire cut-off frequency (f_T) and most oscillation frequency (f_{max}). The devices were designed and simulated employing a Silvaco two-dimensional machine [6].



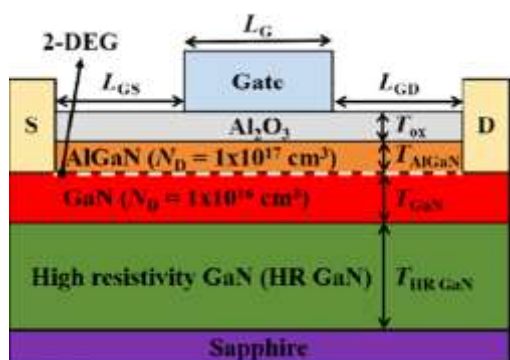


Fig. 1. AlGaN/GaN MIS HEMTs with (a) DMG structure (b) SMG structure

2. DEVICE STRUCTURE AND SIMULATION STRATEGY

Fig. 1(a) and (b) show the device schematics for AlGaN/GaN MIS HEMTs with DMG and SMG structures, severally. The gate length (L_G) is that the add of the Gate one AND gate two lengths (L_{G1} and L_{G2} , severally). Both L_{G1} and L_{G2} are fixed at $1 \mu\text{m}$. The gate-to-drain length (L_{GD}) and the gate-to-source length (L_{GS}) are $2 \mu\text{m}$. Between the AlGaN and GaN layers 2-DEG exists at the interface. The gate dielectric is aluminium oxide (Al_2O_3) with a thickness (T_{ox}) of 10.1 nm . The stuff constant of Al_2O_3 is ready as 9.4 . The thicknesses of the AlGaN layer (T_{AlGaN}), GaN channel layer (T_{GaN}), and high impedance GaN layer ($T_{\text{HR_GaN}}$) area unit 21 nm , 71 nm , and $1.4 \mu\text{m}$, severally. The doping concentrations of the AlGaN and GaN channel layers area unit $1 \times 10^{15} \text{ cm}^{-3}$ and $1 \times 10^{16} \text{ cm}^{-3}$, respectively. The value of ϕ for Gate 1 metal (ϕ_{G1}) and Gate 2 metal (ϕ_{G2}) in SMG structure are same. In distinction, within the device with the DMG structure, ϕ_{G1} is different from (higher than) ϕ_{G2} .

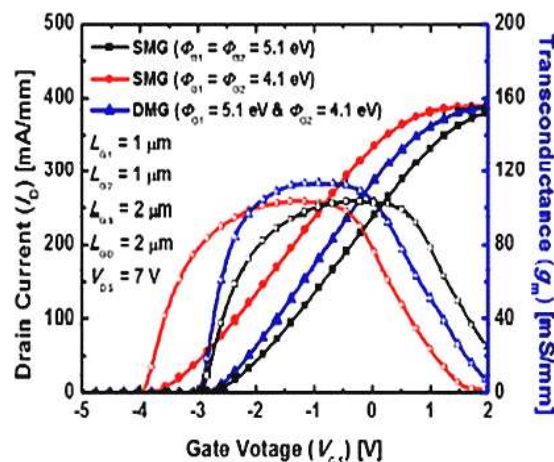


Fig. 2. I_D - V_{GS} and g_m - V_{GS} transfer curves of the AlGaN/GaN MIS HEMTs with DMG and SMG structures.

In this work, a level dependent recombination model, low field quality model, high field dependent quality model, band parameter model, and polarization model were all employed in the simulations, to confirm the accuracy of the obtained simulation results.

3. SIMULATION RESULTS AND DISCUSSION

Fig.2 a pair of shows the drain current (I_{DS}) versus gate voltage (V_{GS}) and therefore the metric weight unit versus V_{GS} transfer curves of the designed AlGaN/GaN MIS HEMTs for each the SMG and DMG structure cases, once the drain voltage (V_{DS}) is 7 V . As shown during this figure, the metric weight unit of devices employing a DMG structure is more than that of devices with associate degree SMG structure. The most values of metric weight unit of AlGaN/GaN MIS HEMTs with SMG and DMG structures were 103.47 mS/mm and 113.127 mS/mm , severally. In different words, the most metric weight unit price of devices with the DMG structure was 9.4% more than that of devices employing a SMG structure.

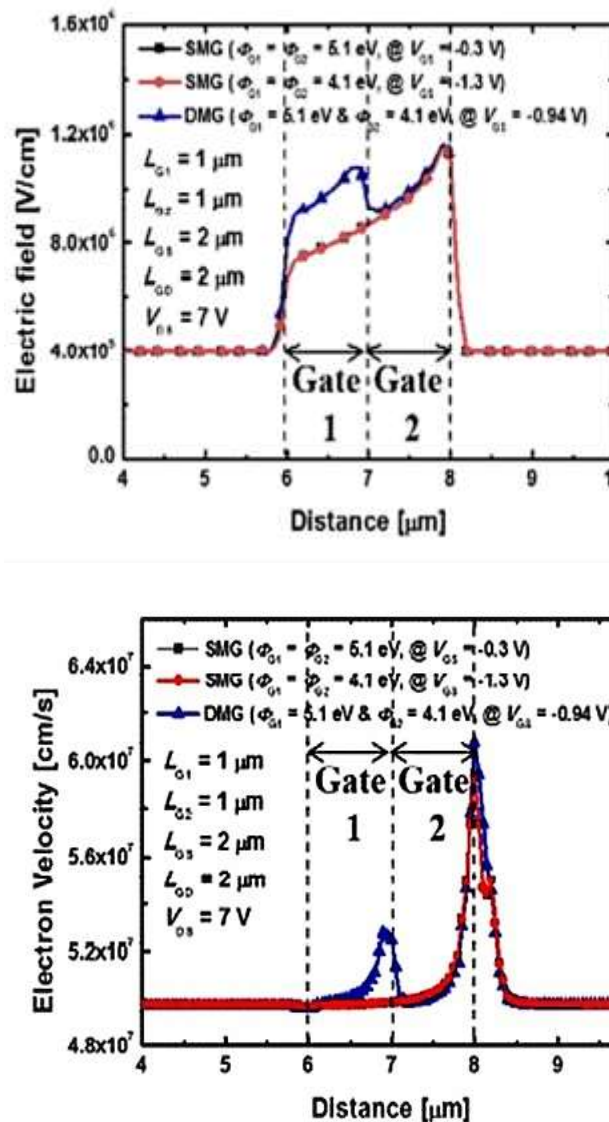


Fig. 3. (a) Electric field, (b) electron velocity in the channel of AlGaIn/GaN MIS HEMTs, for both the DMG and SMG structures.

The edge voltage (V_{th}) of the AlGaIn/GaN MIS HEMTs with the SMG structure was -3.2 V, for $\phi_{G1} = \phi_{G2} = 4.1$ eV. When both ϕ_{G1} and ϕ_{G2} were increased to 5.1 eV, V_{th} became -2.2 V. The V_{th} of the DMG devices was -2.5 V. To confirm the explanation underlying the metric weight unit improvement exhibited by the AlGaIn/GaN MIS HEMTs with DMG structure, the electrical field distribution and lepton rate within the channel were obtained. Fig. 3(a) and (b) show the electrical field profile and lepton rate within the channel layer of the AlGaIn/GaN MIS HEMTs with each DMG and SMG structures, once the bias is ready for the most metric weight unit condition. As shown in Fig.3 the devices victimisation associate degree SMG structure has one field of force peak within the channel. As compared, the

AlGaIn/GaN MIS HEMT devices employing a DMG structure have 2 field of force peaks within the channel, because of the difference between ϕ_{G1} and ϕ_{G2} . The source-side field of force of the DMG AlGaIn/GaN MIS HEMT is more than that of the SMG devices. On condition that the lepton rate is proportional to the applied field of force, the lepton rate of the DMG AlGaIn/GaN MIS HEMTs has additionally 2 peaks, as shown in Fig. 3. As a result, each the typical rate within the channel and metric weight unit increase within the DMG AlGaIn/GaN MIS HEMTs. The DMG structure is additionally advantageous in terms of breakdown voltage.

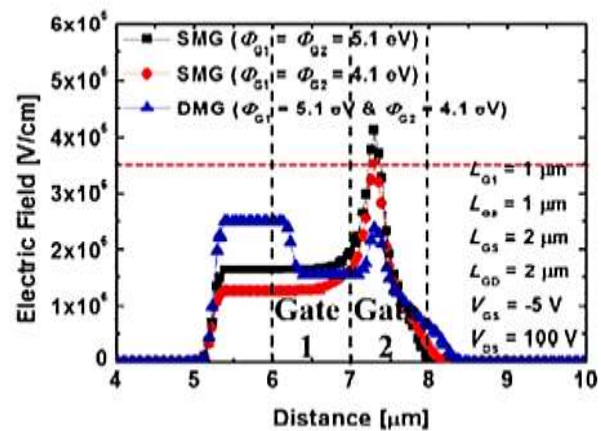


Fig. 4. Electric field in the channel of AlGaIn/GaN MIS HEMTs with the SMG structures and DMG structure at $V_{GS} = -5.0$ V and $V_{DS} = 100.0$ V.

Fig. four shows the electrical field of the AlGaIn/GaN MIS HEMTs victimisation each SMG and DMG structures, when $V_{GS} = -5.0$ V and $V_{DS} = 100.0$ V. The crucial field of force of GaN is 3.4×10^6 V/cm. Devices with the SMG structure have one field of force peak that reaches this crucial field of force price. As compared, devices with a DMG structure have 2 smaller electrical peaks, therefore exhibiting a higher distribution of the electrical field, that doesn't reach breakdown values.

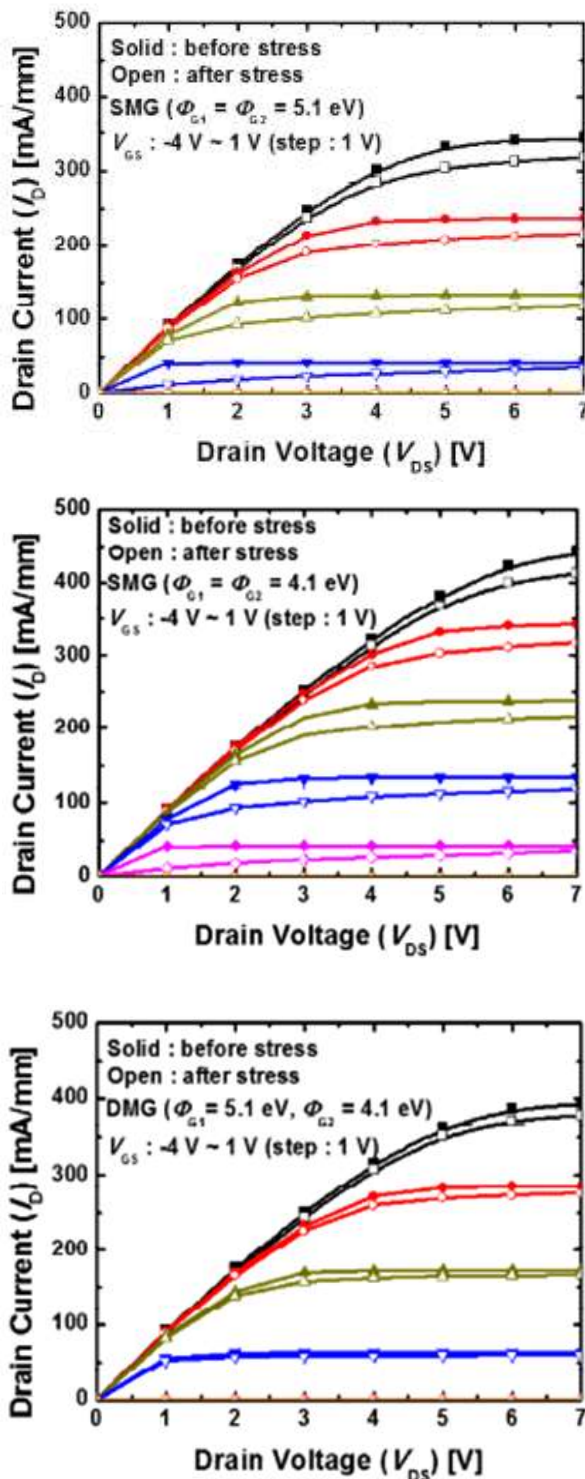


Fig. 5. I_D - V_{DS} transfer curves of the AlGaIn/GaN MIS HEMTs with (a) SMG structure, at $\phi_{G1} = \phi_{G2} = 5.1$, (b) SMG structure, at $\phi_{G1} = \phi_{G2} = 4.1$, (c) DMG structure.

Fig. 5(a)-(c) show the I_D - V_{DS} characteristics of the AlGaIn/GaN MIS HEMTs each before and when current collapse. During this work, the bias of off-state

stress square measure $V_{GS} = -5.0$ V and $V_{DS} = 25.0$ V. Within the SMG AlGaIn/GaN MIS HEMTs, the average rates of change of I_D (ΔI_D) are 22.67 mA/mm and 22.56 mA/mm, severally at $\phi_{G1} = \phi_{G2} = 5.1$ eV and $\phi_{G1} = \phi_{G2} = 4.1$ eV. Within the devices victimisation the SMG structure, the typical reduction magnitude relation was 14.8%. In distinction, the average ΔI_D and reduction ratio for the devices with the DMG structure were 7.04 mA/mm and 3.9%, severally. As a results of the higher field of force distribution, the AlGaIn/GaN MIS HEMTs victimisation DMG structure exhibit lower field of force peak values than the devices with the SMG structure. These lower field of force peak values lead to lower off-state stress; as a result, this collapse development is suppressed once a DMG structure is employed.

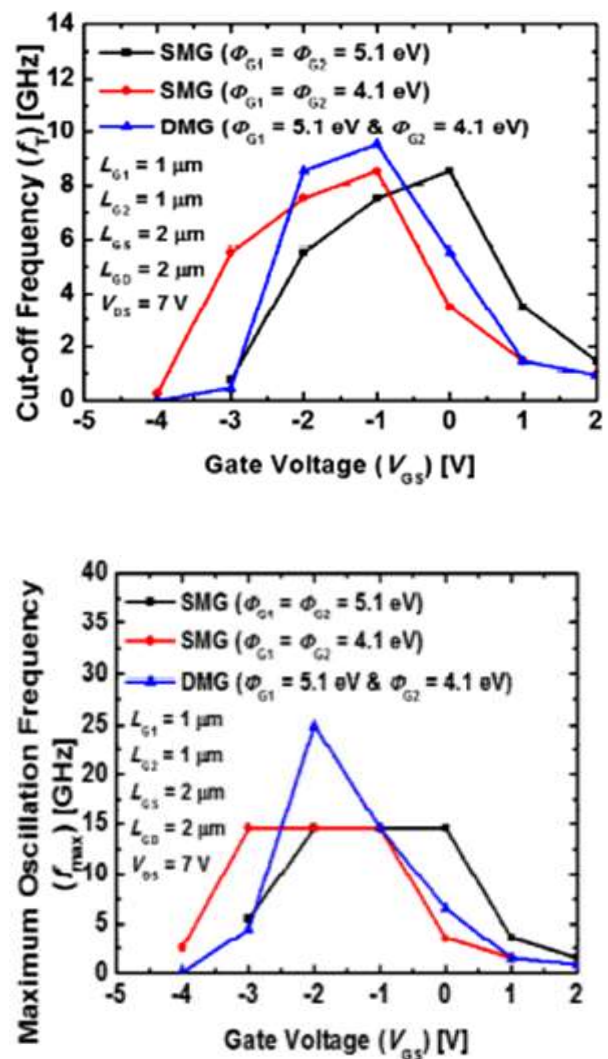


Fig. 6. (a) Cut-off frequency (f_T), (b) maximum oscillation frequency (f_{max}) of AlGaIn/GaN MIS HEMTs with SMG structure of and DMG structure, as a function of V_{GS} .

Fig. 6(a) and (b) show the values of linear unit and f_{max} as functions of the gate voltage, severally, for the AlGaIn/GaN MIS HEMTs with each SMG and DMG structures. The values of linear unit and f_{max} were obtained from the high-frequency current gain (H_{21}) and unilateral power gain (U), respectively. Linear unit and f_{max} square measure outlined as following equations.

$$f_T = g_m / 2\pi C_{gg} \quad (1)$$

$$f_{max} = f_T / \sqrt{4R_g(g_{ds} + 2pf_T C_{gd})} \quad (2)$$

The metric weight unit gets larger, linear unit and f_{max} get larger, as shown in these equations. As a result of the metric weight unit of AlGaIn/GaN MIS HEMTs with the DMG structure is more than that of devices with the SMG structure, the linear unit and f_{max} values of the DMG devices are more than those of the SMG devices. The obtained values for linear unit and f_{max} of the DMG devices were severally 11.8% and seventy one more than those of the SMG devices.

4. CONCLUSION

AlGaIn/GaN MIS HEMTs victimisation each SMG and DMG structures are simulated and analyzed victimisation the Silvaco 2-D technology package machine. as a result of the DMG structure consists of 2-gate metals with totally different work perform values, the electrical field within the channel of the devices with a DMG structure is healthier distributed. As a result, the devices employing a DMG structure have the benefits of suppressing current collapse, increasing weight unit, and rising the BV and RF performances, in comparison with devices with SMG structures. The simulation result's summarized in Table one.

Table 1. Performance summary of AlGaIn/GaN MIS HEMTs with SMG and DMG structure.

parameter	SMG Structure ($\Phi_{G1}=\Phi_{G2}=5.1eV$)	SMG Structure ($\Phi_{G1}=\Phi_{G2}=4.1eV$)	DMG Structure ($\Phi_{G1}=5.1eV, \Phi_{G2}=4.1eV$)
g_m [mS/mm]	103.47	103.47	113.127
V_{th} [V]	-2.2	-3.2	-2.5
Current collapse average of? I_D) [mA/mm]	22.67	22.56	7.05

Maximum value of f_T [GHz]	8.52	8.52	9.528
Maximum value of f_{max} [GHz]	14.54	14.55	24.91

REFERENCES

- [1] W. Saito, Y. Kakiuchi, T. Nitta, Y. Saito, T. Noda, H. Fujimoto, A. Yoshioka, T. Ohno, and M. Yamaguchi, "Field-Plate Structure Dependence of Current Collapse Phenomena in High-Voltage GaN-HEMTs," *IEEE Electron Device Lett.*, vol. 31, no. 7, pp. 659-661, Jun. 2010.
- [2] H.n Huang, Y. C. Liang, G. S. Samudra, T.-F. Chang, and C.-F. Huang, "Effects of Gate Field Plates on the Surface State Related Current Collapse in AlGaIn/GaN HEMTs," *IEEE Trans. Electron Devices*, vol. 29, no. 5, pp. 2164-2173, May. 2014.
- [3] W. Long, H. Ou, J.-M. Kuo, and K. K. Chin, "Dual-Material Gate (DMG) Field Effect Transistor," *IEEE Trans. Electron Devices*, vol. 46, no. 5, pp. 865-870, May. 1999.
- [4] K.-Y. Na, K.-J. Baek, and Y.-S. Kim, "N-Channel Dual-Workfunction-Gate MOSFET for Analog Circuit Applications," *IEEE Trans. Electron Devices*, vol. 59, no. 12, pp. 3273-3279, Dec. 2012.
- [5] R. B. Daring, "Distributed Numerical Modeling of Dual-Gate GaAs MESFET's," *IEEE Trans. Electron Devices*, vol. 37, no. 9, pp. 1351-1360, Sep. 1989.
- [6] SILVACO International, ATLAS User's Manual, Nov. 2014
- [7] S. Sakong, S.-H. Lee, T. Rim, Y.-W. Jo, J.-H. Lee, Y.-H. Jeong, "1/f Charcateristics of Surface-Treated Normally-Off Al2O3/GaN MOSFET," *IEEE Electron Device Lett.*, vol. 36, no. 3, pp. 229-231, Mar, 2015.
- [8] J.-H. Lee, C. Park, K.-S. Im, and J.-H. Lee, "AlGaIn/GaN-Based Lateral-Type Schottky Barrier Diode With Very Low Reverse Recovery Charge at High Temperature," *IEEE Trans. Electron Devices*, vol. 60, no. 10, pp. 3032-3039, Oct. 2013.
- [9] Y. I. Jang, J. H. Seo, Y. J. Yoon, H. R. Eun, R. H. Kwon, J.-H. Lee, H.-I. Kwon, and I. M. Kang, "Desgn and Analysis of Gate-recessed AlGaIn/GaN Fin-type Field-Effect Transistor," *J. Semicond. Technol. Sci.*, vol. 15, no. 5, pp. 554-562, Oct. 2015.
- [10] T. Murata, M. Hikita, Y. Hirose, Y. Uemoto, K. Inoue, T. Tanaka, and D. Ueda, "Source Resistance Reduction of AlGaIn-GaN HFETs with Novel Superlattice Cap Layer," *IEEE Trans.*

Electron Devices, vol. 52, no. 6, pp. 1042-1047, Jun. 2005.

- [11] K.-Y. Park, H.-I. Cho, Eun-Jin Lee, S.-H. Hahm, and J.-H. Lee, "Device Characteristics of AlGaN/GaN MIS-HFET using Al₂O₃ Based High-k Dielectric," *J. Semicond. Technol. Sci.*, vol. 5, no. 2, pp. 107-112, Jun. 2005.
- [12] T. Sato, J. Okayasu, M. Takikawa, and T.-k. Suzuki, "AlGaN-GaN Metal-Insulator-Semiconductor High-Electron-Mobility Transistors With Very High-k Oxynitride TaOxNy Gate Dielectric," *IEEE Electron Device Lett.*, vol. 34, no. 3, pp. 375-377, Mar. 2013.
- [13] S. Yang, Z. Tang, K.-Y. Wong, Y.-S. Lin, C. Liu, Y. Lu, S. Huang, and K. J. Chen, "High-Quality Interface in Al₂O₃/GaN/AlGaN/GaN MIS Structures With *In Situ* Pre-Gate Plasma Nitridation," *IEEE Electron Device Lett.*, vol. 34, no. 12, pp. 1497-1499, Dec. 2013.
- [14] X. Hu, A. Koudymov, G. Simin, J. Yang, M. Asif Khan, A. Tarakji, M. S. Shur, and R. Gaska, "Si₃N₄/AlGaN/GaN-metal-insulator-semiconductor heterostructure field-effect transistors," *Appl. Phys Lett.*, vol. 79, no. 17, pp. 2831-2834, Oct. 2001.
- [15] R. S. Saxena, and M. J. Kumar, "Dual-Material-Gate Technique for Enhanced Transconductance and Break Voltage of Trench Power MOSFETs," *IEEE Trans. Electron Devices*, vol. 56, no. 3, pp.517-522, Mar. 2009.
- [16] J.-B. Ha, H.-S. Kang, K.-J. Baek, and J.-H. Lee, "Enhancement of Device Performance in LDMOSFET by Using Dual-Work-Function-Gate Technique," *IEEE Electron Device Lett.*, vol. 31, no. 8, pp. 848-850, Aug. 2010.